journal

J. Am. Ceram. Soc., 95 [9] 2965–2971 (2012)
DOI: 10.1111/j.1551-2916.2012.05261.x
© 2012 The American Ceramic Society

Combined Structural and Quantitative Texture Analysis of Morphotropic Phase Boundary $Pb(Mg_{1/3}Nb_{2/3})O_3$-$PbTiO_3$ Ceramics

Harvey Amorín,[‡,†] Daniel Chateigner,[§] Janez Holc,[¶] Marija Kosec,[¶] Miguel Algueró,[‡] and Jesús Ricote[‡]

[‡]Department of Materials for Information Technologies, Instituto de Ciencia de Materiales de Madrid, CSIC, Cantoblanco, 28049 Madrid, Spain

[§]UMR 6508 CRISMAT Laboratory, ENSICAEN/CNRS, Université de Caen-Basse Normandie, F-14050 Caen, France

[¶]Electronic Ceramics Department, Jožef Stefan Institute, Jamova 39, 1000 Ljubljana, Slovenia

The combination of the quantitative texture analysis and Rietveld methods is used to study the preferential orientation of morphotropic phase boundary (MPB) $Pb(Mg_{1/3}Nb_{2/3})O_3$-$PbTiO_3$ ceramics obtained by homogeneous Templated Grain Growth. Their complex structure, with the coexistence of several polymorphs, and the presence of texture that is required to take advantage of their excellent piezoelectric properties, raise serious problems for a precise characterization of these materials. Conventional methods of texture analysis, although simple, are limited, and the information obtained, if not studied with care, may be misleading. The use of linear detectors and χ-scan are more appropriate for the study of diffraction peaks with several contributions as it is the case for MPB compositions. This work shows the simultaneous determination of structural and texture parameters through the application of the so-called combined method, already used for the analysis of similar problems in a range of polycrystalline materials, to this specific case.

I. Introduction

Preferential crystallographic orientation, or texture, has become a fundamental parameter in the study of polycrystalline anisotropic materials with enhanced functionalities, as the development of a certain degree of texture is essential to take advantage of the highest values of the properties of individual crystals along specific directions. A good example of this type are ferroelectric materials, where considerable effort has been made to obtain highly textured ceramics, with the objective to approach the piezoelectric coefficients reported for single crystals.[1] To this aim, textured ferro/piezoelectric ceramics have been prepared by templated grain growth (TGG),[2–10] in which preferential crystallographic orientation is achieved through the growth of well aligned templates at the expense of a surrounding fine-grained matrix during sintering.[1]

Crystalline phases showing ultrahigh piezoelectric coefficients along specific crystallographic directions have attracted special attention, like $(1-x)Pb(Mg_{1/3}Nb_{2/3})O_3$-$xPbTiO_3$ (PMN-PT).[5–10] One specific issue related to them is that these large coefficients appear only for compositions close to the morphotropic phase boundary (MPB) between rhombohedral and tetragonal polymorphs, and therefore any phase deviation must be controlled. To complicate things, high aspect ratio PMN-PT templates, needed for an effective alignment previous to the TGG process, are not available yet, and anisometric crystals of other compositions have mostly been used.[5–8] Nevertheless, the use of templates of the same phase is preferred, and cube-shaped PMN-PT microcrystals have been proved to be a successful alternative.[9,10] Therefore, the evaluation of the degree of orientation and of any phase deviation is crucial in this case to develop PMN-PT ceramics with the highest piezoelectric coefficients possible.

However, the simplest and most routinely used method to characterize texture; the Lotgering analysis of conventional X-ray diffraction (XRD) patterns, seems not good enough to provide the characterization required. The Lotgering factor, which is defined as 0 for a randomly oriented and 1 for a fully textured material, is obtained from the comparison of the relative intensities of the diffraction peaks with those of a randomly oriented material.[11] This method is heavily dependent on the 2θ range used for calculations,[12] and it is only a qualitative factor to compare texture among different samples, for a specific crystallographic direction perpendicular to the sample surfaces. No information can be obtained about the angular distribution of this orientation, which is a more important parameter that defines the quality of the texture achieved in TGG ceramics.

Rocking curves are used for this purpose, and by their analysis using the March–Dollase equation two texture parameters are defined: the *volume fraction of oriented material* and the *degree of texture* which characterizes the width of the angular distribution of orientations.[13] This is an adequate method for materials exhibiting axisymmetric texture profiles with the symmetry axis along the main specimen direction, also called cyclic-fiber textures, which is the type of texture developed in textured ceramics obtained under uniaxial stress fields.[1,14–16] However, for ceramics with compositions close to a MPB, the coexistence of several polymorphs results in the splitting of the diffraction peaks, which can complicate the interpretation of the results obtained by these conventional methods of texture characterization. This can be partly solved by the use of linear detectors to collect the XRD data, which allows the full peak profiles to be recorded, and thus the subsequent analysis of the integrated intensities.[17]

In any case, the best method to obtain quantitative information of texture is the measurement of pole figures and the subsequent calculation of the orientation distribution (OD) function.[18] The OD function contains complete information of all texture components (in-plane and out-of-plane) and allows the calculation of a global degree of preferential orientation. However, as before, the correct determination of the

S. E. Trolier-McKinstry—contributing editor

Manuscript No. 30432. Received October 04, 2011; approved April 10, 2012.
[†]Author to whom correspondence should be addressed. e-mail: hamorin@icmm.csic.es

texture parameters requires a precise knowledge of the structural parameters of the material, which is usually difficult in highly textured materials, and specifically in materials at MPBs. A solution is the use of the so-called combined approach[19] that, in brief, introduces the quantitative texture analysis into the Rietveld method.[20] This has been proved to be a viable tool,[21] and has successfully been applied to the study of many oriented ceramics and polycrystalline films.[22–24] The advantage is the combination of different analyses of diffraction data to mutual benefit allowing a simultaneous and more precise determination of microstructural and structural parameters at the same time as texture characteristics. This is ideally suited for the analysis of the characteristics of textured 0.65PMN-0.35PT ceramics.

In this work, traditional and advanced methods of texture analysis are used and the results are compared to discuss their differences and the feasibility of their application to the study of textured ceramics of complex oxides at MPBs.

II. Experimental Procedure

To prepare the textured ceramics, a $0.65Pb(Mg_{1/3}Nb_{2/3})O_3$-$0.35PbTiO_3$ powder with a 2 wt% excess of PbO (for introducing a liquid phase during the TGG process)[25] was synthesized by mechanochemical activation of the binary oxides in air with a high-energy planetary mill using WC milling media.[26] Cube-shaped microcrystals of the same composition, with an average size of ~50 μm, were used as templates.[10] Slurries for tape casting were prepared in ethanol (99.7% grade, Panreac, Barcelona, Spain) using PVB, Poly(vinyl butyral) (Aldrich, St. Louis, MO), as binder, and BBP, Benzyl butyl-phthalate (Merck-Schuchardt, Hohenbrunn, Germany) as plasticizer.[10] A 5 wt% of templates was added and stirred for 1 h previous to the tape casting experiments. Slips were cast onto a silicone-coated Mylar™, cut, stacked and laminated under an uniaxial pressure of 10 MPa for 15 min. Organics were burned out at 500°C for 2 h in air. Finally, TGG was carried out at 1150°C for 10 h using heating/cooling rates of 5°C/min in closed alumina crucibles. Samples were wrapped in Pt foils and embedded in a $PbZrO_3$ powder with a 5 wt% excess of PbO, which creates the necessary PbO-rich atmosphere to limit weight losses and the formation of pyrochlore during sintering.[25] Besides the textured ceramics obtained by this method, randomly oriented ceramics were prepared from the same powder by sintering at 1200°C for 1 h in $PbZrO_3$ powder using heating/cooling rates of 3°C/min. Density was evaluated from their weight and dimensions.

Microstructure was characterized using a Field Emission Gun Scanning Electron Microscope (FEG-SEM, Nova NanoSEM 230 microscope, FEI Company, Hillsboro, OR) on cross-sections perpendicular to the casting plane, as indicated in Fig. 1. Sample was prepared by polishing with Al_2O_3 suspensions to 0.1 μm, and by thermal etching at 800°C for 20 min and then quenching down to room temperature. The volume fraction of TGG material was obtained from the area fraction occupied in the images by analyzing a large cross-section of ~3 mm^2, which includes more than 100 grown templates. Image analysis was carried out with a computerized system (MIP45, Digital Image Systems S.L., Barcelona, Spain).

Conventional XRD experiments were carried out on polished ceramics, using a Siemens D500 (Munich, Germany) diffractometer and CuK_α radiation. Data were collected in the 2θ range from 20 to 70° in steps of 0.05° with an integration time of 5 s/step. These data were used to calculate the Lotgering factor[11] corresponding to the $\langle 001\rangle_p$-crystallographic orientation perpendicular to the sample surface (using pseudocubic indices). Rocking curve and pole figures were obtained using a Huber 4-circle goniometer (Rimsting, Germany) mounted on a X-ray generator (CuK_α radiation) and equipped with a curved position-sensitive detector (Model CPS-120, Inel, Artenay, France),[19] covering an angle of 120° range in 2θ (angular resolution of 0.03°). All these experiments were carried out on 15 mm × 15 mm surfaces parallel to the casting plane, with a beam size of 1 mm × 1 mm cross-section, which, for the incident angle used, represents an irradiated area of around 3 mm × 1 mm. The configuration of the measurement is schematically shown in Fig. 1.

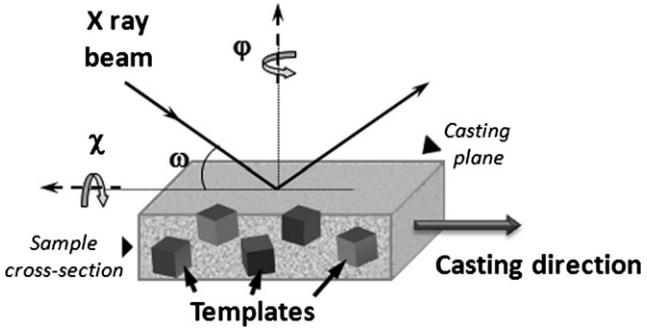

Fig. 1. Configuration of the measurement, which schematically relates the casting direction and cubic-shaped templates arrangement with the X-ray incident angle (ω) and the rotation angles (χ, ϕ).

Rocking curve measurements were carried out around the 002 diffraction peak (2θ ≈ 45.15°) and varying the incidence angle ω in steps of 0.5° with integration times of 150 s/step. The modified March-Dollase function, Eq. (1), was used to extract two texture parameters from its fitting to the experimental data: the volume fraction of oriented material (f_v) and the degree of orientation (r)[13]: In this case, f_v refers to the fraction of oriented TGG material; i.e. extensive growth of templates showing preferred orientation about the axis perpendicular to the casting plane. The strength of preferred orientation is given by r ($0 < r < 1$): $r = 1$ corresponds, in our case, to a set of crystals with their pseudocubic $\langle 001\rangle_p$ directions distributed at random, while $r = 0$ appears for a material with all crystals perfectly aligned with their $\langle 001\rangle_p$ directions perpendicular to the casting plane.

$$F(f_v, r, \omega) = f_v \left(r^2 \cos^2\omega + \frac{\sin^2\omega}{r} \right)^{-\frac{3}{2}} + (1 - f_v) \qquad (1)$$

X-ray diagrams at different sample orientations were measured varying the tilt angle (χ) between 0 and 60° in 1° steps, with integration times of 150 s/step.

Fiber texture perpendicular to the casting plane is assumed, and the rotation angle (ϕ) was varied continuously to obtain average values in all experiments. The casting process only produces an orientation of the templates perpendicular to the casting plane, but not in the casting direction (see Fig. 1). Templates align within the laterally homogenous, vertical (perpendicular to the casting plane) shear gradient under the blade, and so only out-of-plane orientation results.[1,27] Previous reports show that, with the appropriate processing parameters, cubic microcrystals can also be successfully aligned during forming by tape casting and produce fiber textures.[9,10]

The analysis of the diffraction data is carried out by the so-called combined approach.[19] Briefly, an iterative Rietveld refinement and texture analysis of the series of X-ray diagrams measured at different sample orientations is carried out. First, each diagram is modeled using the usual (ω, χ, ϕ)-dependent Rietveld formulation, and compared to the experimental data. The calculated diagrams are adjusted to observations using a nonlinear least-squares minimization technique. Then, preferred orientation factors in each diagram are obtained from integrated intensities, which are extracted using the texture-adapted Le Bail approach,[28] a method to obtain integrated intensities of individual reflec-

tions from powder diagrams with a large number of overlaps. Calculated intensities are obtained from an initial OD function, OD: f(**g**), with **g** = {α,β,γ}, Euler angles (Matthies convention).[29] The initial calculated intensity values are forced to the same weight, i.e. 1 (for a randomly oriented sample). During the successive iterations the least-squares procedure forces the respective intensities to become coherent with the observed overlap, and progressively converge to the observed intensities. The extracted intensities are then finally obtained for the best fit, and serve as the initial texture factor for the next OD refinements. From the several methods of resolution, we chose the entropy modified E-WIMV (Williams-Imhof-Matthies-Vinel) iterative method.[30] The OD cell values are computed through an entropy iteration algorithm. Once this process is finished, a new Rietveld analysis is carried out, and after several cycles calculations converge to a final result.

The OD function f(**g**) represents the volumetric density of crystallites oriented in $d\mathbf{g}$. It is measured in m.r.d. (multiple of a random distribution) and normalized to the value $f_r(\mathbf{g}) = 1$ m.r.d. for a sample without any preferred orientation. The normalization condition is that the integral of f(**g**) over the whole orientation space is equal to $8\pi^2$. Pole figures can be calculated from the OD and are expressed in m.r.d., a unit of the OD densities and that is equivalent to vol% per 1% area. In such units, a sample without preferred orientations exhibits uniform pole figures with 1 m.r.d. levels, while a textured sample shows pole figures with maxima and minima of orientation densities ranging from 0 m.r.d. (absence of crystals oriented in this direction) to infinity (for a single crystal on few directions). The overall texture strength is evaluated through the texture index: $F^2 = (1/8\pi^2)\Sigma_i\{[f(g_i)]^2\Delta g_i\}$, being the i orientation cells. It varies from 1 (random powder) to infinity (perfect texture or single crystal) and it is used to compare the texture strength of different samples exhibiting similar ODs. Texture components are deduced from the calculated inverse pole figures, these latter being calculated from the f(**g**) for a given sample direction (**y**) and representing the distribution of crystal directions relative to **y**. The quality of the refinements (Rietveld and E-WIMV) is assessed by the reliability factors R_{wp} (weighted profile), R_B (Bragg) and GoF (Goodness of Fit). Calculations were carried out with the Materials Analysis Using Diffraction package (MAUD).[31]

III. Results and Discussion

The successful application of the TGG method to the processing of 0.65PMN-0.35PT ceramics is demonstrated in the SEM image of a cross-section perpendicular to the casting plane (Fig. 2). Large blocky grains with a reduced amount of fine-grained matrix among them are observed, which indicates the extensive growth of the templates achieved at the expense of the matrix. The final average crystal size is about 100 μm, which is twice the size of the initial templates. The volume fraction occupied by the grown crystals f_v was estimated to be 0.73 from the area fraction occupied by them in several FEG-SEM images. This provides a direct measure of the volume fraction of TGG material. The successful TGG process is also reflected on the ceramic relative density, which is above 93% of the theoretical value.

Regarding the crystallographic texture obtained, conventional XRD data (Fig. 3) clearly show the preferential orientation achieved for the TGG ceramic when compared with a randomly oriented, unseeded ceramic obtained by conventional sintering. No significant phase deviations are expected, as the splitting of the diffraction peaks (see inset of Fig. 3), characteristic of MPB compositions, is clearly exhibited. The Lotgering factor associated to the $h00$ diffraction peaks was calculated from the integrated intensity of all peaks in a large enough 2θ range (20–70°), to get the most reliable value possible.[12] In our case, no significant change in f_{h00} was obtained

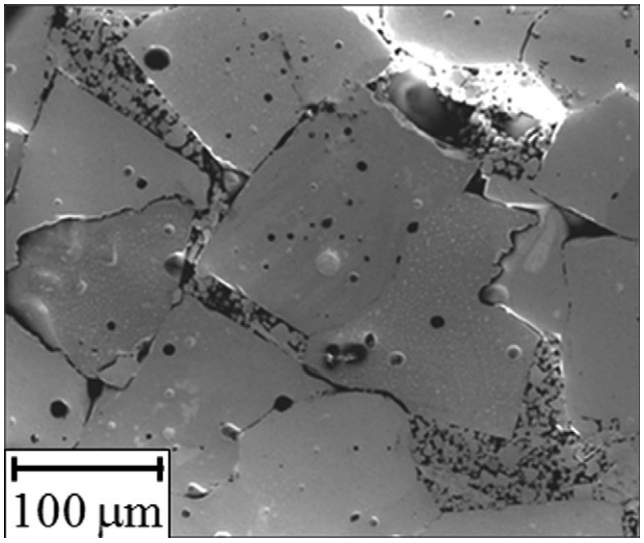

Fig. 2. FEG-SEM micrograph of a cross-section perpendicular to the casting plane of a TGG 0.65PMN-0.35PT ceramic.

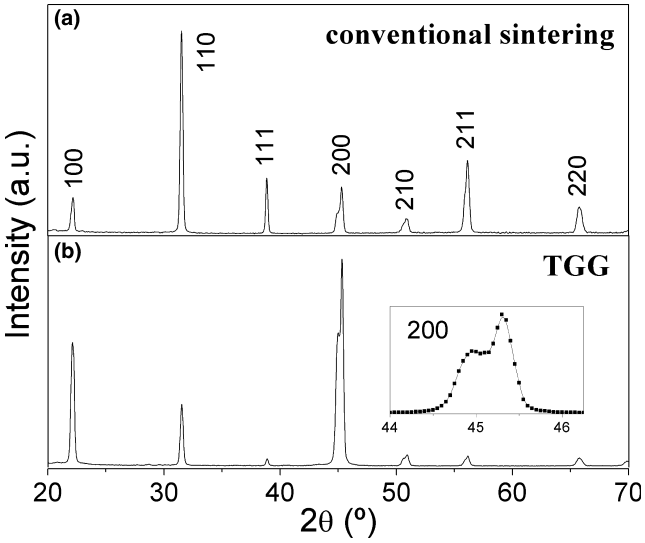

Fig. 3. XRD patterns of 0.65PMN-0.35PT ceramics: (a) conventional sintering and (b) TGG.

by considering the peaks above 70° in 2θ. The result is a value of $f_{h00} = 0.78$ which indicates texturing achieved with the $\langle 001 \rangle_p$ direction mainly perpendicular to the casting plane. The overlap has not been resolved here, thus a pseudocubic cell was assumed.

More information on the texturing efficiency of the TGG process can be obtained from a study of the variation of the diffraction intensities when the sample is studied under different angles. Figure 4 presents the results of these studies around the 200 Bragg peak: ω-scan (conventional rocking curve) and χ-scan (incidence angle ω is kept constant and the sample is tilted around an axis located in the sample plane). The two experiments are in principle equivalent for cyclic-fiber texture, as it is expected for our oriented ceramics, but the latter (χ-scan) is not as limited in angle range as the conventional rocking curve (a maximum ± 20° in most cases), which makes it more adequate for the analysis of wider angular distributions.

This is clearly seen in Fig. 4(a), where the 200 rocking curve of a randomly oriented ceramic is shown together with the corresponding χ-scan. In the rocking curve, it must be

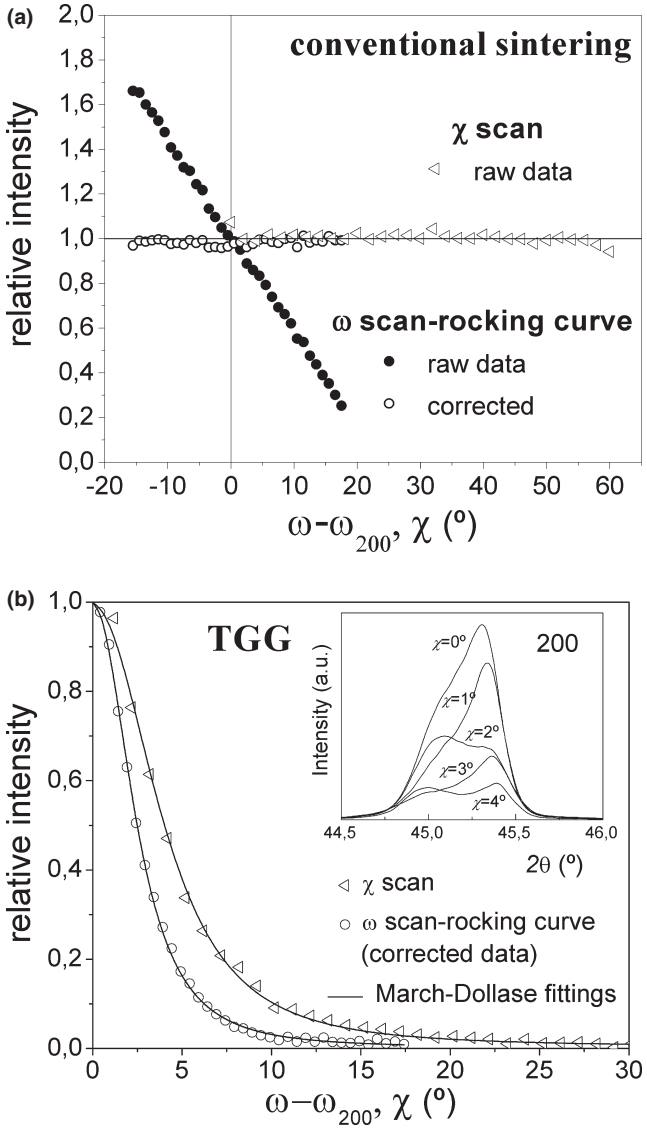

Fig. 4. 200 rocking curves and χ-scans measurements of 0.65PMN-0.35PT ceramics: (a) conventional sintering and (b) TGG. ω_{200} is the incidence angle at which is fulfilled the Bragg condition for $\{200\}_p$ planes perpendicular to the sample surface.

considered that the diffracted intensity of the experimental raw data (solid circles) can be affected by defocusing and volume-absorption effects, which is corrected as reported elsewhere,[19] and results are shown in the figure (open circles). However, this is not necessary in χ-scan, as intensities only start to be affected significantly by defocusing at angles above 60°.

When both measurements are carried out on the textured ceramic [see Fig. 4(b)] we obtain Full Widths at Half Maximum (FWHM) of 5.8 and 8.2° for rocking curve and χ-scan, respectively. The March–Dollase equation is fit to the experimental data (with a goodness of fit $R^2 > 0.997$) and provides the texture parameters collected in Table I. From the rocking curve corrected data we obtain: $r = 0.147$ and $f_v = 0.6$. The χ-scan results give: $r = 0.208$ and $f_v = 0.69$. The values of the texture parameter r are in the range of the ones reported for other TGG ceramics that were processed with anisometric templates.[6,15,16] This demonstrates that cubic microcrystals can successfully be used to process high-quality textured ceramics of perovskite oxides by a homogenous-TGG. The discrepancy observed in the r values obtained from both methods can be explained due to the differences of both experiments.

Table I. Texture Parameters Obtained from Conventional Techniques of Analysis for a Textured 0.65PMN-0.35PT Ceramic

Technique	f_v	r
Lotgering method	0.78†	–
FEG-SEM analysis	0.73	–
Rocking curves	0.6 ± 0.3‡	0.147 ± 0.002‡
χ-scan curves	0.69 ± 0.11‡	0.208 ± 0.001‡

†In this case the value refers to the Lotgering factor, f_{h00}.
‡March–Dollase fit (goodness of fit $R^2 > 0.997$).

The χ-scans study the evolution of the integrated intensity of the diffraction peaks at the same incidence angle; therefore, we are analyzing the same type of crystallographic planes at different tilt angles. This is important when we analyze an MPB composition with the complex split peaks as the one that can be seen in the inset of Fig. 4(b). Rocking curves change instead the incidence angle, as the objective is the determination of the maximum angle at which we observe similar misoriented planes with respect to the sample surface, but still fulfilling the Bragg condition. The results of this experiment are more difficult to discuss when complex diffraction peaks are analyzed. This fact supports once again that the more traditional methods are not adequate for the study of textured ceramics of oxides close to MPBs.

It must be noted at this point that we are using a linear detector to perform these scans. This allows us both the study of the evolution of the diffraction peaks as the sample is rotated and the use of the integrated intensity of the whole peak for the calculations. This is especially important in the case of MPB compositions, for which the different contributions present produce complex diffraction peaks. This is the case for 200 of PMN-PT, whose evolution for small variations of the tilt angle χ can be seen in the inset of Fig. 4(b). Note that only if the integrated intensity of the whole peak is considered a meaningful rocking curve or χ-scan is obtained. The use of a point detector in this case may otherwise produce misleading results.

With all these considerations, conventional methods of analysis of the XRD data produce a consistent set of texture parameters summarized in Table I. According to the previous discussion, χ-scans using linear detectors are the most adequate tools for texture analysis of MPB PMN-PT ceramics. However, none of these methods is able to provide precise information on the structural characteristics of the MPB compositions, regardless of the importance of phase deviations for the final properties of the ceramics.

The only available solution is the use of the combined method of analysis that allows the simultaneous study of the structural characteristics and texture. Figure 5 shows an example of the application of this combined method through a series of XRD diagrams measured with a curved (linear) position-sensitive detector at increasing tilt angles (χ). Both experimental variations in diffraction peaks intensities (due to texture), and corresponding Rietveld fits are shown. It can be seen that experimental data are nicely reproduced. A mixture of monoclinic (space group *Pm*) and tetragonal (*P4mm*) polymorphs of MPB PMN-PT has been considered herein,[32] using the crystallographic information files n° 1 501 475 and 1 501 476 from the Crystallography Open Database,[33] to obtain better reliability factors for the Rietveld analysis (GoF = 1.5). Considering only the tetragonal *P4mm* or the monoclinic *Pm* phases in the refinement gave larger GoFs (2.5 and 1.8, respectively). In any case, according to the results of the refinement, the textured ceramic is above 99% monoclinic *Pm*. In addition, the presence of residual PbO secondary phase is found to be residual. This indicates the almost complete consumption of the PbO by the TGG process at the final stages of the sintering. The value is so small

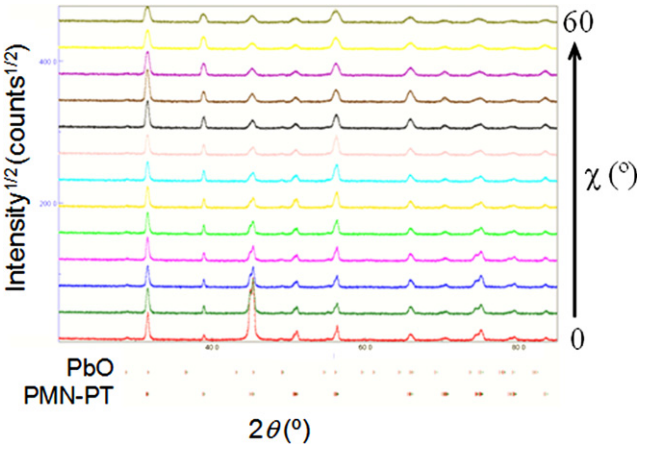

Fig. 5. Experimental (dotted line) and fitted (solid line) XRD diagrams for increasing χ angles of a TGG 0.65PMN-0.35PT ceramic. The refinement was carried out combining Rietveld and E-WIMV analysis. Peak positions for the two phases analyzed are indicated.

that it cannot be considered relevant, but it is necessary to refine the data with the best reliability factors as possible.

The structural parameters obtained for both the randomly oriented and textured ceramics are summarized in Table II. When compared with the reference values of a PMN-PT powder with a composition containing a slightly larger amount of PT: 0.64PMN-0.36PT[32] (also added in the Table), a slight increase of a and b lattice parameters, accompanied with a decrease of c and β, is observed. This is in agreement with the tendencies followed by these parameters when the amount of PT is increased in the monoclinic phase close to the boundary with the tetragonal phase (see fig. 10 of Reference 34) and, therefore, gives a firm evidence that no significant deviations have appeared in the phase composition of these ceramics during processing, and crystals have the crystalline structure corresponding to the MPB.

The combined analysis not only provides us with structural data, but also texture is quantitatively determined through the OD function, obtained with reliability factors as low as $R_{wp} = 4.4\%$ and $R_B = 6.4\%$ for the textured ceramic (Table II). The texture index $F^2 = 32$ m.r.d.^{2} is a high value for this coefficient as compared to similar ceramics and elaboration techniques,[14,23,35] that corresponds to the strength of the global orientation of the TGG processed ceramic. This is the first report of this coefficient in a textured PMN-PT ceramic, a number that includes all the components of texture in the ceramic, which can be better visualized in the inverse pole figures, in which a specific direction of the sample is chosen and the crystal directions aligned to it are represented. In our PMN-PT ceramics texture components appear with ⟨100⟩, ⟨010⟩, and ⟨001⟩ monoclinic reciprocal directions perpendicular to the sample surface, as it can be seen in Fig. 6(b) for the TGG processed ceramic. Note the absence of significant directions of texturing in the conventionally sintered ceramic [Fig. 6(a)].

The OD along these crystallographic directions is represented best in their corresponding pole figures, which can be recalculated from the OD for both ceramics (Fig. 7). The lack of texturing results in pole figures with values close to 1 m.r.d. [Fig. 7(a)] while a maximum of 27.5 m.r.d. is obtained for one of the monoclinic directions ⟨001⟩ in the center of the pole figure, i.e. perpendicular to the sample surface [Fig. 7(b)]. As we are using the combined analysis with the Rietveld method and, therefore, we have an accurate determination of the structural parameters, it is possible to deconvolute and separate the {200}, {020}, and {002} pole figures and study them separately. A difference between the maxima of the normalized {002} (27.5 m.r.d.), {200} (19.82 m.r.d.), and {020} (20.25 m.r.d.) pole figures is found. Although the difference is not large, the one associated to the largest lattice parameter c shows the highest distribution density at maximum, which is related to a slightly larger number of crystals oriented this way, which also are aligned more efficiently since the central pole distribution in the {002} pole figure appears narrower than that in the two others. As it is not expected that the alignment of the original template crystals by tape casting produces any preference among these three directions, this is most probably an effect of the mechanical polishing carried out prior to the XRD experiment, which has been widely described in ferroelectric materials.[36]

The use of the combined method, therefore, seems to be the most adequate way to assess a texturing process of ceramics, overall when the crystalline structure plays an important role in the final properties, as it is the case for MPB compositions. In this work we also try to show the cor-

Table II. Structural and Texture Parameters Obtained from the Application of the Combined Method of Analysis for 0.65PMN-0.35PT Ceramics

Structural parameters	a (Å)	b (Å)	c (Å)	β (°)
Monoclinic *Pm*	4.00952(7)	3.99861(5)	4.03671(5)	90.164(2)
Texture	$F^2 = 3$ m.r.d^2			
Conventionally Sintered Ceramic				
Reliability factors				
Rietveld fit	$R_{wp} = 15\%$	$R_B = 11\%$	GoF = 1.3	—
OD refinement	$R_{wp} = 4.9\%$	$R_B = 5.1\%$	—	—
Structural parameters	a (Å)	b (Å)	c (Å)	β (°)
Monoclinic *Pm*	4.00664(6)	3.99814(3)	4.03178(3)	89.7910(13)
Texture	$F^2 = 32$ m.r.d^2			
Tgg Processed Ceramic				
Reliability factors				
Rietveld fit	$R_{wp} = 17\%$	$R_B = 13\%$	GoF = 1.5	—
OD refinement	$R_{wp} = 4.4\%$	$R_B = 6.4\%$	—	—
Structural parameters	a (Å)	b (Å)	c (Å)	β (°)
Monoclinic *Pm*	4.0055(9)	3.9897(8)	4.0426(8)	90.19(2)
Reference data[32] 0.64PMN-0.36PT powder (225 K)				
Reliability factors	$R_{wp} = 7.88\%$	—	GoF = 1.8	—

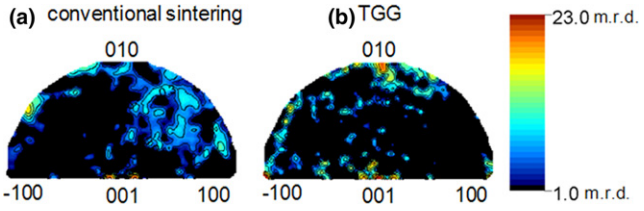

Fig. 6. Inverse pole figures for the normal direction to the sample surface of 0.65PMN-0.35PT ceramics: (a) conventional sintering and (b) TGG. Equal area projection and linear density scale.

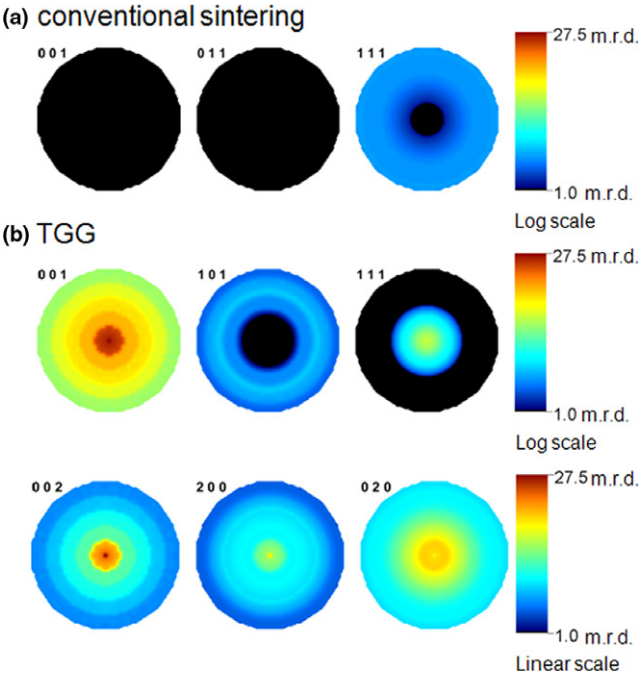

Fig. 7. Reconstructed pole figures of 0.65PMN-0.35PT ceramics: (a) conventional sintering and (b) TGG. Equal area projection.

relation between the crystalline structure and texture, and how the precise determination of one depends on the other. To obtain the lattice parameters of the dominant polymorph of these PMN-PT ceramics is necessary first to correctly quantify the texture induced by the TGG process. Details of the OD function, like the small differences found in the relative orientation along the different monoclinic directions, are only available after a precise determination of the lattice parameters. Besides, the results of this thorough characterization, not available by any of the other conventional techniques, demonstrate the validity of the application of the homogeneous-TGG approach to produce high-quality textured MPB PMN-PT ceramics.

IV. Conclusions

The use of advanced methods of XRD analysis for the characterization of MPB PMN-PT ceramics is essential to precisely characterize the two sets of parameters that largely determine the final properties we pursue: those that describe the crystalline structure and texture. To this end the use of the Rietveld method combined with Quantitative Texture Analysis allows the study of the phases present, lattice parameters, and components of the global texture, simultaneously. This is very relevant for the study of complex oxide ceramics where structural deviations from the desired phase may have important consequences on their behavior, as it is the case of the MPB PMN-PT ceramics analyzed in this work, where texturing is obtained by a novel homogeneous-TGG approach. In this case, the use of PMN-PT templates, instead of anisometric crystals of other phases, has the advantage of not affecting the crystalline structure as the results show. Similar questions are raised in the studies of other systems, like for example alternative lead-free piezoelectric solid solutions, which also seek for the best coefficients around their MPBs, which can benefit from the access to the structural and textural information provided by this combined method of analysis of diffraction data. Besides, the comparison of the results obtained by the different methods of texture analysis carried out in this work, reveals that the use of linear detectors followed by an analysis of the integrated diffracted intensities of the whole peak, particularly the use of χ-scan, is the most appropriate method for the study of complex diffraction peaks, which contain contributions from several phases. Their evolution as the sample is tilted (i.e., for the measurement of a conventional rocking curve) may produce misleading results about the degree of orientation of the ceramic, if it is not properly analyzed.

Acknowledgments

This work was financially supported by MICINN (Spain) through projects MAT2010-18543 and MAT2011-23709. Dr. H. A. thanks support by the MICINN Programme "Ramón y Cajal". Dr. D.C. acknowledges the Conseil Régional de Basse Normandie for partial financial of the X-ray instrument for Combined Analysis. The authors are grateful to Dr. Mai Pham Thi (Thales Res. & Tech. France) for providing the templates and to Prof. Rodrigo Moreno and Ms. Tamara Molina (ICV-CSIC, Spain) for support in the processing of the materials.

References

[1]G. L. Messing, S. Trolier-McKinstry, E. M. Sabolsky, C. Duran, S. Kwon, B. Brahmaroutu, P. Park, H. Yilmaz, P. W. Rehrig, K. B. Eitel, E. Suvaci, M. M. Seabaugh, and K. S. Oh, "Templated Grain Growth of Textured Piezoelectric Ceramics," *Crit. Rev. Solid State Mater. Sci.*, **29**, 45–96 (2004).

[2]Y. Saito, H. Takao, T. Tani, T. Nonoyama, K. Takatori, T. Homma, T. Nagaya, and M. Nakamura, "Lead-Free Piezoceramics," *Nature*, **432**, 84–7 (2004).

[3]H. Amorín, A. L. Kholkin, and M. E. V. Costa, "Texture Development and Dielectric Properties of $SrBi_2Ta_2O_9$ Ceramics Processed by Templated Grain Growth," *J. Eur. Ceram. Soc.*, **25** [12] 2453–6 (2005).

[4]Y. Chang, S. Poterala, Z. Yang, and G. L. Messing, "Enhanced Electromechanical Properties and Temperature Stability of Textured $(K_{0.5}Na_{0.5})NbO_3$-Based Piezoelectric Ceramics," *J. Am. Ceram. Soc.*, **94** [8] 2494–8 (2011).

[5]S. Kwon, E. M. Sabolsky, G. L. Messing, and S. Trolier-McKinstry, "High Strain, ⟨001⟩ Textured $0.675Pb(Mg_{1/3}Nb_{2/3})O_3$-$0.325PbTiO_3$ Ceramics: Templated Grain Growth and Piezoelectric Properties," *J. Am. Ceram. Soc.*, **88** [2] 312–7 (2005).

[6]K. H. Brosnan, S. F. Poterala, R. J. Meyer, S. Misture, and G. L. Messing, "Templated Grain Growth of < 001 > Textured PMN–28PT using $SrTiO_3$ Templates," *J. Am. Ceram. Soc.*, **92** [S1] S133–9 (2009).

[7]Y. Yan, K.-H. Cho, and S. Priyaw, "Templated Grain Growth of ⟨001⟩-Textured $0.675Pb(Mg_{1/3}Nb_{2/3})O_3$-$0.325PbTiO_3$ Piezoelectric Ceramics for Magnetic Field Sensors," *J. Am. Ceram. Soc.*, **94** [6] 1784–93 (2011).

[8]S. F. Poterala, S. Trolier-McKinstry, R. J. Meyer Jr, and G. L. Messing, "Processing, Texture Quality, and Piezoelectric Properties of $\langle 001 \rangle_C$ Textured $(1\text{-}x)Pb(Mg_{1/3}Nb_{2/3})TiO_3$-$xPbTiO_3$ Ceramics," *J. Appl. Phys.*, **110**, 014105, 8pp (2011).

[9]M. Pham-Thi, H. Hemery, O. Durand, and H. Dammak, "Orientation Distribution and Fiber Texture of Highly Oriented Piezoceramics: $(1\text{-}x)PbMg_{1/3}Nb_{2/3}O_3$-$xPbTiO_3$ System," *Jpn. J. Appl. Phys.*, **43** [12] 8190–4 (2004).

[10]H. Amorín, I. Santacruz, J. Holc, M. P. Thi, M. Kosec, R. Moreno, and M. Alguero, "Tape-Casting Performance of Ethanol Slurries for the Processing of Textured PMN-PT Ceramics from Nanocrystalline Powder," *J. Am. Ceram. Soc.*, **92** [5] 996–1001 (2009).

[11]F. K. Lotgering, "Topotactical Reactions with Ferrimagnetic Oxides having Hexagonal Crystal Structures - I," *J. Inorg. Nucl. Chem.*, **9** [2] 113–23 (1959).

[12]J. L. Jones, E. B. Slamovich, and K. J. Bowman, "Critical Evaluation of the Lotgering Degree of Orientation Texture Indicator," *J. Mater. Res.*, **19** [11] 3414–22 (2004).

[13]W. A. Dollase, "Correction of Intensities for Preferred Orientation in Powder Diffractometry - Application of the March Model," *J. Appl. Crystallogr.*, **19**, 267–72 (1986).

[14]D. Chateigner and J. Ricote, "Quantitative Texture Analysis of Polycrystalline Ferroelectrics"; pp. 347–408 in *Multifunctional Polycrystalline Ferroelectric Materials*, Chapter 8, Springer Series in Materials Science 140. Edited by L. Pardo and J. Ricote. Springer, Dordrecht, 2011.

[15]M. M. Seabaugh, M. D. Vaudin, J. P. Cline, and G. L. Messing, "Comparison of Texture Analysis Techniques for Highly Oriented α-Al_2O_3," *J. Am. Ceram. Soc.*, **83** [8] 2049–54 (2000).

[16]K. H. Brosnan, G. L. Messing, R. J. Meyer, and M. D. Vaudin, "Texture Measurements in ⟨001⟩ Fiber-Oriented PMN-PT," *J. Am. Ceram. Soc.*, **89** [6] 1965–71 (2006).

[17]H.-J. Bunge, H.-R. Wenk, and J. Pannetier, "Neutron-Diffraction Texture Analysis using a 2-Theta-Position Sensitive Detect," *Texture Microstruct.*, **5** [3] 153–70 (1982).

[18]H.-J. Bunge, *Texture Analysis in Materials Science: Mathematical Methods*. Butterworths, London, U.K., 1982.

[19]D. Chateigner, *Combined Analysis: Structure-Texture-Microstructure-Phase-Stresses-Reflectivity Analysis by X-Ray and Neutron Scattering*. 496 pp. Wiley-ISTE, London, 2010, ISBN: 978-1-84821-198-8.

[20]H.-R. Wenk, S. Matthies, and L. Lutterotti, "Texture Analysis from Diffraction Spectra," *Mater. Sci. Forum*, **157–162**, 473–9 (1994).

[21]S. Matthies, L. Lutterotti, and H.-R. Wenk, "Advances in Texture Analysis from Diffraction Spectra," *J. Appl. Crystall.*, **30**, 31–42 (1997).

[22]J. Ricote and D. Chateigner, "Quantitative Microstructural and Texture Characterization by X-Ray Diffraction of Polycrystalline Ferroelectric Thin Films," *J. Appl. Crystallogr.*, **37**, 91–5 (2004).

[23]E. Guilmeau, D. Chateigner, J. Noudem, R. Funahashi, S. Horii, and B. Ouladdiaf, "Rietveld Texture Analysis of Complex Oxides: Examples of Polyphased Bi2223 Superconducting and Co349 Thermoelectric Textured Ceramics Characterization Using Neutron and X-Ray Diffraction," *J. Appl. Crystallogr.*, **38**, 199–210 (2005).

[24]S. Deniel, N. Tessier-Doyen, C. Dublanche-Tixier, D. Chateigner, and P. Blanchart, "Processing and Characterization of Textured Mullite Ceramics from Phyllosilicates," *J. Eur. Ceram. Soc.*, **30** [12] 2427–34 (2010).

[25]H. Amorín, J. Ricote, J. Holc, M. Kosec, and M. Algueró, "Homogeneous Templated Grain Growth of $0.65Pb(Mg_{1/3}Nb_{2/3})O_3$-$0.35PbTiO_3$ from Nanocrystalline Powders Obtained by Mechanochemical Activation," *J. Eur. Ceram. Soc.*, **28** [14] 2755–63 (2008).

[26]D. Kuscer, J. Holc, and M. Kosec, "Formation of $0.65Pb(Mg_{1/3}Nb_{2/3})O_3$-$0.35PbTiO_3$ using a High-Energy Milling Process," *J. Am. Ceram. Soc.*, **90** [1] 29–35 (2007).

[27]H. J. Kim, M. J. M. Krane, K. P. Trumble, and K. J. Bowman, "Analytical Fluid Flow Models for Tape Casting," *J. Am. Ceram. Soc.*, **89** [9] 2769–75 (2006).

[28]A. Le Bail, "Whole Powder Pattern Decomposition Methods and Applications: A Retrospection," *Powder Diffr.*, **20** [4] 316–27 (2005).

[29]H. R. Wenk, S. Matthies, J. Donovan, and D. Chateigner, "BEARTEX: a Windows-Based Program System for Quantitative Texture Analysis," *J. Appl. Crystallogr.*, **31**, 262–9 (1998).

[30]Y. S. Liu, F. Wang, J. Z. Xu, and Z. Liang, "Estimation of the True Orientation Distribution Function Determination of the Maximum-Entropy Method by the Taylor Model," *J. Appl. Crystallogr.*, **26**, 268–71 (1993).

[31]L. Lutterotti, S. Matthies, H.-R. Wenk, A. J. Schultz, and J. Richardson, "Texture and Structure Analysis of Deformed Limestone from Neutron Diffraction Spectra," *J. Appl. Phys.*, **81** [2] 594–600 (1997). Freeware available at http://www.ing.unitn.it/~maud/ (accessed 28 September 2011).

[32]A. K. Singh, D. Pandey, and O. Zaharko, "Powder Neutron Diffraction Study of Phase Transitions in and a Phase Diagram of $(1-x)Pb(Mg_{1/3}Nb_{2/3})O_3$-$xPbTiO_3$," *Phys. Rev. B*, **74** [2] 024101, 18pp (2006).

[33]S. Grazulis, D. Chateigner, R. T. Downs, A. F. T. Yokochi, M. Quiros, L. Lutterotti, E. Manakova, J. Butkus, P. Moeck, and A. Le Bail, "Crystallography Open Database - An Open-Access Collection of Crystal Structures," *J. Appl. Crystallogr.*, **42**, 726–9 (2009).

[34]A. K. Singh and D. Pandey, "Evidence for M_B and M_C Phases in the Morphotropic Phase Boundary Region of $(1-x)[Pb(Mg_{1/3}Nb_{2/3})O_3]$-$xPbTiO_3$: A Rietveld Study," *Phys. Rev. B*, **67**, 064102, 12pp (2003).

[35]E. Guilmeau, H. Itahara, T. Tani, D. Chateigner, and D. Grebille, "Quantitative Texture Analysis of Grain-Aligned $[Ca_2CoO_3](0.62)[CoO_2]$ Ceramics Processed by the Reactive-Templated Grain Growth Method," *J. Appl. Phys.*, **97** [6] 064902, 7pp (2005).

[36]M. F. Wong and K. Zeng, "Mechanical Polishing Effects Toward Surface Domain Evolution in $Pb(Zn_{1/3}Nb_{2/3})O_3$-$PbTiO_3$ Single Crystals," *J. Am. Ceram. Soc.*, **94** [4] 1079–86 (2011). □